Separation Science and Technology
Publication details, including instructions for authors and subscription information:
http://www.informaworld.com/smpp/title~content=t713708471

Groundwater Cleanup by In-Situ Sparging. X. Air Channeling Model for Biosparging of Nonaqueous Phase Liquid

David J. Wilson[a]; Robert D. Norris[a]; Ann N. Clarke[a]
[a] ECKENFELDER INC., NASHVILLE, TENNESSEE, USA

To cite this Article Wilson, David J. , Norris, Robert D. and Clarke, Ann N.(1996) 'Groundwater Cleanup by In-Situ Sparging. X. Air Channeling Model for Biosparging of Nonaqueous Phase Liquid', Separation Science and Technology, 31: 10, 1357 — 1376
To link to this Article: DOI: 10.1080/01496399608001401
URL: http://dx.doi.org/10.1080/01496399608001401

SEPARATION SCIENCE AND TECHNOLOGY, 31(10), pp. 1357–1376, 1996

Groundwater Cleanup by In-Situ Sparging. X. Air Channeling Model for Biosparging of Nonaqueous Phase Liquid

DAVID J. WILSON, ROBERT D. NORRIS, and ANN N. CLARKE
ECKENFELDER INC.
227 FRENCH LANDING DRIVE, NASHVILLE, TENNESSEE 37228, USA

ABSTRACT

A column model is developed to simulate the removal and biodegradation of dissolved and nonaqueous phase liquid (NAPL) volatile organic compounds (VOCs) from contaminated aquifers by biosparging. The model assumes that the injected air moves through the aquifer in persistent channels and that NAPL must dissolve and move to these channels by diffusion and dispersion. The dependence of model results on several of the parameters of the model is investigated, and suggestions for optimizing biosparging system operations are made. The removal of NAPL VOCs of quite low solubility (such as alkanes) from smear zones below the water is modeled, and is found to be an extremely slow process. Drawing down the water table to below the smear zone by pumping is suggested as a possible solution.

INTRODUCTION

In-situ techniques for the remediation of contaminated soil and groundwater at UST sites and hazardous waste sites have been very helpful in reducing the massive costs of these cleanups. One of the most common challenges confronting the environmental engineer is the remediation of groundwater and associated soils which are contaminated with volatile and/or biodegradable organic compounds such as chlorinated solvents, hydrocarbons, and oxygenated compounds such as alcohols and ketones. Pump and treat methods, the usual prescription in the past, have been quite ineffective at most of the sites at which they have been tried (1),

plagued by the slow rate of mass transport by diffusion from porous domains of low permeability and by the slow rate of solution of droplets of nonaqueous phase liquids if NAPLs are involved.

Sparging and biosparging techniques, in which air is injected into the aquifer below the zone of contamination, show considerable promise for further reducing the costs of in-situ remediation of contaminated groundwater (2, 3). Volatile contaminants are partitioned into the air as it rises through the aquifer, and are then normally captured by an associated soil vapor extraction system. If the contaminants are biodegradable, their destruction by microbial action is greatly enhanced by the increased oxygen concentrations in the aquifer and vadose zone which result from sparging. When sparging systems are managed to maximize the contribution to remediation by biodegradation, we describe the process as biosparging.

Biosparging has two advantages over straight sparging if the VOCs to be removed are biodegradable: 1) The total volume of air required in biosparging is substantially less than that required for sparging. 2) The VOC concentrations in the off-gas are reduced, sometimes to the point where off-gas recovery by soil vapor extraction (SVE) and treatment are not required. SVE will be required, of course, if nearby buildings, sewer lines, etc. must be protected from infiltration of explosive or toxic vapors.

The advantages of utilizing microbial activity in SVE have been known for some time, and bioventing has been employed at a large number of petroleum-contaminated sites. Hinchee and Ong (4) developed an in-situ respirometric test for measuring biodegradation rates, and the general field of bioremediation was reviewed by Hoeppel and Hinchee (5). Kindred and Celia explored mass transport considerations in connection with biodegradation (6), and various mathematical models for bioventing have been developed (Ref. 7, for example).

The conceptual complexity of bioremediation techniques makes them a challenge to model. One must include advective transport in the gas and possibly the liquid phase, and diffusion, dispersion, and possibly desorption kinetics must be modeled. Sufficient water must be present in the soil. The dependence of microbial growth and die-off on substrate (and possibly cosubstrate) concentration), the concentration of dissolved oxygen (or other electron acceptors), and the concentrations of nutrients (nitrogen, phosphorus) and toxins contribute to the rate of the overall process. Such complexity dictates that models employ simple geometry, that they be implemented by complex, slow computer programs, and, perhaps most damaging, that a large number of parameters be evaluated, estimated, or guessed at before the models can be used. Nevertheless, such models are useful tools to evaluate the relative importance of these param-

eters and to identify which parameters should be controlled to optimize performance.

It has recently been demonstrated that the air injected into an aquifer by a sparging well moves through persistent channels up to the water table, rather than as isolated, random bubbles (8, 9). This has major implications for the modeling of sparging and biosparging, in that mass transport of VOC from the aqueous phase to the air channels and of oxygen from the air channels through the aqueous phase are likely to be important rate-limiting factors (10) and must therefore be included in such models. The problem of poor mass transport is exacerbated by demonstrations that water circulation is enhanced only during the start-up and shut-down periods, with virtually no water circulation being induced by steady, continuous sparging (11, 12). A number of workers have suggested that pulsed operation of sparging wells should result in enhanced dispersive mass transport of contaminants and oxygen and therefore in improved rates of remediation (9, 11–14). Movement of water at the onset and termination of a pulse has been demonstrated (11, 12), and an analysis of the effect of pulsed operation on the dispersivity has been given (14).

The results of the simple in-situ respirometric test developed by Hinchee and Ong (4) for bioventing and used at several Air Force bases were successfully interpreted in terms of a relatively simple model in which only biomass, substrate, and oxygen were considered (15). This suggests that one might be able to employ a similar simplification of the modeling of biological processes in biosparging. We here develop such a model, using one-dimensional (column) geometry, air channeling, and a dispersivity which is selected to take into account enhancement resulting from pulsed operation of the sparging well. The analysis is followed by results of calculations done with the model to show the effects of the various parameters.

ANALYSIS

The model includes the following features.

- Air movement is assumed to take place through persistent channels in the otherwise water-saturated porous medium. One of these channels and the surrounding porous medium is represented by means of a cylindrical domain with the air channel located along its axis.
- VOC and oxygen transport in the aqueous phase are assumed to take place by dispersion, with the dispersivity controlled by the pulse duty cycle of the sparging well.

- NAPL droplets may be present; if so, they are assumed to be uniformly distributed throughout the domain of interest. Although uniform distribution is unlikely, one rarely has sufficiently detailed information about a site to improve on this assumption. The solution rate of the droplets is controlled by molecular diffusion through a surrounding stagnant aqueous boundary layer.
- Biodegradation and biomass growth are represented by Monod-type factors in the biomass concentration, the substrate concentration, and the dissolved oxygen concentration, together with an inhibition factor to represent possible toxicity of the substrate at sufficiently high concentrations. The effects of other nutrients (cosubstrates, nitrate, phosphate, etc.) are ignored. Bacterial die-off is assumed to be first order in the biomass concentration.
- Biomass and NAPL droplets are assumed to be stationary.
- Mass transport between the vapor and aqueous phases is assumed to be limited by dispersion in the aqueous phase adjacent to the air/water interface. Local equilibrium of VOC and of oxygen between the liquid and gas phase is assumed at the boundary, with VOC and oxygen obeying Henry's law.
- It is assumed that no longitudinal movement of the aqueous phase takes place.
- It is assumed that, over the range of pressures encountered, air can be regarded as incompressible.

With these assumptions, the analysis leading to the various terms in the equations is straightforward, and much of it was presented earlier in detail (7, 13, 14, 16). Rather than deriving the model equations, therefore, we simply write them down, identifying the physical or biological process which generates each term. The system being analyzed is illustrated schematically in Fig. 1; one of the volume elements shown in this figure is magnified and more detail given about the mathematical partitioning of the system in Fig. 2.

The variables of the system are as follows:

S_{ik}^N = NAPL concentration in the kth annulus of the ith volume element, kg/m^3 of soil

S_{ik}^W = aqueous VOC concentration in the kth annulus of the ith volume element, kg/m^3 of water

O_{ik}^W = dissolved oxygen concentration in the kth annulus of the ith volume element, kg/m^3 of water

B_{ik} = biomass concentration in the kth annulus of the ith volume element, kg/m^3 of soil

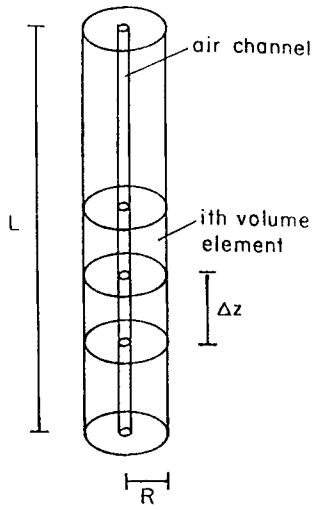

FIG. 1 Geometry of the column model.

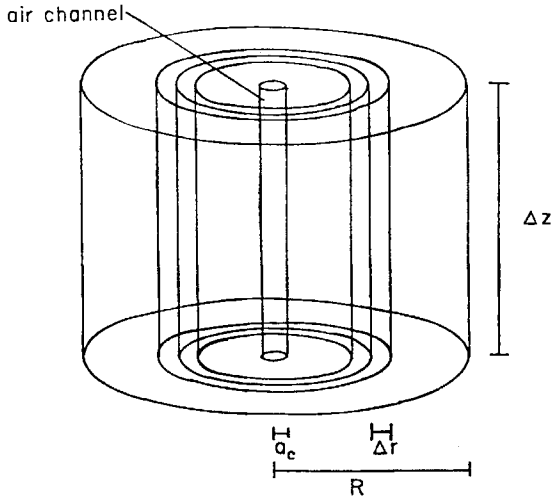

FIG. 2 A volume element in the column model, showing the central air channel and annular volume subelements.

S_i^G = gaseous VOC concentration in the air channel of the ith volume element, kg/m^3 of gas
O_i^G = gaseous oxygen concentration in the air channel of the ith volume element, kg/m^3 of gas

In the model the differential equations controlling the variables (biomass, NAPL, aqueous VOC, dissolved oxygen, gaseous VOC, gaseous oxygen) involve the processes indicated below. Subscripts are omitted here for convenience.

dS^N/dt: solution of droplets
dS^w/dt: solution of droplets, dispersion transport, mass transport between aqueous and vapor phase, biodegradation
dO^w/dt: mass transfer from gas phase (channels), dispersion, biodegradation
dB/dt: formation from substrate consumption, die-off
dS^G/dt: advection in the channel, mass transfer to the aqueous phase
dO^G/dt: advection in the channel, mass transfer to the aqueous phase

We first examine the rate of solution of NAPL droplets. This is assumed to be controlled by diffusion from the droplet through a quiescent boundary layer into the surrounding dispersing water. The equation governing the NAPL concentration is then given by

$$\frac{dS_{ik}^N}{dt} = -\frac{3S_0^N D_f (S_{\text{sat}}^W - S_{ik}^W)(S_{ik}^N/S_0^N)^{1/3}}{a_0^2 \rho_{\text{voc}}[1 - (a_0/d)(S_{ik}^N/S_0^N)^{1/3}}} \tag{1}$$

where S_0^N = initial NAPL concentration, kg/m^3 of soil
D_f = diffusivity of VOC, m^2/s
S_{sat}^W = aqueous solubility of VOC, kg/m^3
a_0 = initial NAPL droplet radius, m
$d - a_0$ = droplet boundary layer thickness, m
ρ_{voc} = density of NAPL, kg/m^3

This equation assumes solution of NAPL occurs by steady-state diffusion of VOC across the boundary layer surrounding the droplet.

If solution kinetics are limiting, $S_{ik}^W \ll S_{\text{sat}}^W$, so can be neglected in Eq. (1). The resulting equation is readily integrated, and a solution kinetics-limited lower bound to the cleanup time can be calculated. The result is

$$t_{1b} = \frac{\rho_{\text{voc}} a_0^2 (3/2 - a_0/b)}{3S_{\text{sat}}^W D_f} \tag{2}$$

if nonaqueous phase liquid is present in the aquifer.

The biomass concentration is assumed to be governed by the following Monod-like equation:

$$\frac{dB_{ij}}{dt} = K_u \frac{B_{ik}}{1 + B_{ik}/B_0} \frac{O_{ik}^W/O_0}{1 + O_{ik}^W/O_0} \frac{S_{ik}^W/S_0}{1 + S_{ik}^W/S_0} \frac{1}{1 + (S_{ik}^W/S_1)^n} - k_{\text{die}} B_{ik} \tag{3}$$

The first term on the right represents Monod kinetics with the last factor corresponding to substrate inhibition; the second term represents die-off. For later use we abbreviate the first term as

$$\text{Growth}_{ik} = K_u \frac{B_{ik}}{1 + B_{ik}/B_0} \frac{O_{ik}^W/O_0}{1 + O_{ik}^W/O_0} \frac{S_{ik}^W/S_0}{1 + S_{ik}^W/S_0} \frac{1}{1 + (S_{ik}^W/S_1)^n} \tag{4}$$

where K_u = maximum possible first-order growth rate, s^{-1}
B_0, O_0, and S_0 = Monod kinetics half-saturation concentrations
S_1 = half-inhibition substrate concentration
n = sharpness-of-onset exponent in substrate inhibition term
k_{die} = die-off first-order rate constant, s^{-1}

All concentrations are in kg/m^3.

The equations governing the dissolved VOC concentrations are the following.

$$\frac{dS_{ik}^W}{dt} = -(1/v)\frac{dS_{ik}^N}{dt} + \frac{2\pi \Delta z D_s}{v \Delta v_k \Delta r} \times [r_k(S_{i,k-1}^W - S_{ik}^W) + r_{k+1}(S_{i,k+1}^W - S_{ik}^W)] - (n_s/v)\,\text{Growth}_{ik},$$
$$k = 2, 3, \ldots, n_r - 1 \tag{5}$$

where R = radius of column, m
n_r = number of annuli into which a volume element is partitioned
a_c = radius of air channel, m
$\Delta r = (R - a_c)/n_r$, m
L = length of column, m
n_s = number of volume elements into which the column is partitioned
$\Delta z = L/n_z$
$r_k = a_c + (k - 1)\Delta r$
$\Delta v_k = \pi \Delta z (r_{k+1}^2 - r_k^2)$

At the outer boundary of the volume element,

$$\frac{dS_{i,nr}^W}{dt} = -(1/v)\frac{dS_{i,nr}^N}{dt} + \frac{2\pi \Delta z D_s}{v \Delta v_{nr} \Delta r} r_{nr}(S_{i,nr-1}^W - S_{i,nr}^W) - (n_s/v)\text{Growth}_{i,nr} \tag{6}$$

At the boundary of the channel we have

$$\frac{dS_{i,1}^W}{dt} = -(1/v)\frac{dS_{i,1}^N}{dt} + \frac{2\pi\Delta z D_s}{v\Delta v_1 \Delta r}[2r_1(S_i^G/K_H - S_{i1}^W) + r_2(S_{i2}^W - S_{i1}^W)] - (n_s/v)\text{Growth}_{i1} \quad (7)$$

where K_H = Henry's constant of VOC, dimensionless
D_s = dispersivity, m^2/s

The equations for dissolved oxygen are as follows. For $k = 2, 3, \ldots, n_r - 1$:

$$\frac{dO_{ik}^W}{dt} = \frac{2\pi\Delta z D_s}{v\Delta v_k \Delta r}[r_k(O_{i,k-1}^W - O_{ik}^W) + r_{k+1}(O_{i,k+1}^W - O_{ik}^W)] - (n_0/v)\text{ Growth}_{ik} \quad (8)$$

At the outer boundary of the column:

$$\frac{dO_{i,nr}^W}{dt} = \frac{2\pi\Delta z D_s}{v\Delta v_{nr}\Delta r} r_{nr}(O_{i,nr-1}^W - O_{i,nr}^W) - (n_0/v)\text{Growth}_{i,nr} \quad (9)$$

At the boundary of the air channel:

$$\frac{dO_{i1}^W}{dt} = \frac{2\pi\Delta z D_s}{v\Delta v_1 \Delta r}[2r_1(O_i^G/K_{H0} - O_{i1}^W) + r_2(O_{i2}^W - O_{i1}^W)] + (n_0/v)\text{Growth}_{i1} \quad (10)$$

In the air channel itself the VOC and oxygen concentrations are governed by the equations

$$\frac{dS_i^G}{dt} = \frac{1}{v\pi a_c^2 \Delta z}\left[q_{air}(S_{i-1}^G - S_i^G) - \frac{2\pi\Delta z r_1 D_s}{\Delta r/2}(S_i^G/K_H - S_{i1}^W)\right] \quad (11)$$

and

$$\frac{dO_i^G}{dt} = \frac{1}{v\pi a_c^2 \Delta z}\left[q_{air}(O_{i-1}^G - O_i^G) - \frac{2\pi\Delta z r_1 D_s}{\Delta r/2}(O_i^G/K_{H0} - O_{i1}^W)\right] \quad (12)$$

where q_{air} = air flow rate, m^3/s. The inlet gaseous oxygen and VOC concentrations O_0^G and S_0^G are set equal to 0.2786 kg/m^3 and zero, respectively.

The total residual mass of VOC in the column at time t is given by

$$M_{tot}(t) = \sum_{i=1}^{n_z}\left\{\left[\sum_{k=1}^{n_r}\Delta v_k(S_{ik}^N + vS_{ik}^W)\right] + va_c^2\pi\Delta z S_i^G\right\} \quad (13)$$

The mass of VOC removed by volatilization at time t is accumulated during the course of the run by means of Eq. (14).

$$M_{\text{vol}}(t + \Delta t) = M_{\text{vol}}(t) + q_{\text{air}} S_{nz}^{G}(t) \Delta t \tag{14}$$

The mass of VOC destroyed by biodegradation at time t is given by

$$M_{\text{bio}}(t) = M_{\text{tot}}(0) - M_{\text{tot}}(t) - M_{\text{vol}}(t) \tag{15}$$

In carrying out computations with the model it was found that rather small values of Δt must be used to avoid numerical instability in the solutions to the differential equations. We therefore used the steady-state approximation for the gas-phase concentrations, an approach used earlier by Gomez-Lahoz et al. (16) in a bioventing model. One merely sets the left-hand sides of Eqs. (11) and (12) equal to zero and solves the resulting equations for S_i^G and O_i^G, respectively. The resulting algebraic equations are

$$S_i^G = \frac{q_{\text{air}} S_{i-1}^G + (4\pi \Delta z r_1 D_s / \Delta r) S_{i1}^W}{q_{\text{air}} + (4\pi \Delta z r_1 D_s / \Delta r K_{\text{H}})} \tag{16}$$

and

$$O_i^G = \frac{q_{\text{air}} O_{i-1}^G + (4\pi \Delta z r_1 D_s / \Delta r) O_{i1}^W}{q_{\text{air}} + (4\pi \Delta z r_1 D_s / \Delta r K_{\text{H0}})} \tag{17}$$

Use of the steady-state approximation permitted an increase in Δt by a factor of ten, with a corresponding decrease in computer time per run.

In an earlier paper (14) a method was given for estimating the effective dispersivity resulting from pulsed operation of a sparging well. We present here an alternative approach which appears equally plausible and gives a rather similar answer. The argument is as follows.

Let

ΔL = variation in the height of the water table during the course of a pulse cycle
Δt = duration of a complete pulse cycle
δ = grain size parameter characteristic of the porous medium

When air flow in the sparging well is initiated, the water in the surrounding aquifer is rising, moving generally parallel to the air channels. A measure of its velocity is

$$v = \frac{\Delta L}{\Delta t/2} \tag{18}$$

We are interested in the component of the dispersion which is perpendicular to the air channels, so require the transverse dispersivity, D_{T}.

According to Scheidegger (17), this can be estimated as

$$D_T = D_{molec} + \alpha_T \delta v \tag{19}$$

where D_T = transverse dispersivity
D_{molec} = molecular diffusivity
$\alpha_T = 0.055$

When D_{molec} is neglected, this gives for the transverse dispersivity

$$D_T = 2 \times 0.055\ \delta \Delta L / \Delta t \tag{20}$$

We select representative values of the parameters, $\delta = 0.1$ cm, $\Delta L = 10$ cm, and $\Delta t = 10$ minutes. These yield a value for D_T of 1.8×10^{-8} m^2/s, about 100 times larger than the molecular diffusivity and of the same order as our previous estimate of the dispersivity. From Eq. (20) we see that large values of ΔL (the mounding parameter) and small values of Δt (the duration of the duty cycle of the pulsed sparging well) give the largest values of the dispersivity. This suggests that pulsed sparging wells be run at relatively high air pressures, a conclusion identical to that reached in our earlier analysis.

RESULTS

The model was implemented in TurboBASIC and run on MMG 386-SX (16 MHz) and 386-DX (33 MHz) microcomputers equipped with math coprocessors. A typical 50-day simulation required about 27 minutes on the faster machine.

The VOCs selected for use in the simulations are toluene, a contaminant of some concern which is of relatively high solubility in water, and *n*-octane, to represent volatile aliphatic compounds, the solubilities of which are a good deal lower than those of the BTEX compounds (benzene, toluene, ethylbenzene, xylenes). The properties of these two hydrocarbons and their stoichiometric ratios for combustion with oxygen are given in Table 1.

Typically, the ratio of substrate hydrocarbon mass consumed to biomass formed is around 2. We therefore choose $n_s = 2$. We assume that the oxygen required per kilogram of biomass produced is equal to that needed to convert the required mass of substrate (2 kg) to carbon dioxide and water, permitting us to neglect endogenous respiration. This reasoning gives $n_0 = 6.26$ for toluene and $n_0 = 7.00$ for *n*-octane, values which we regard as reasonable but hardly definitive. Gomez-Lahoz et al. (16) summarized information on this point. Our values of n_0 were selected to provide enough oxygen to permit mineralization of biomass after death, since we are not including an endogenous respiration term explicitly.

TABLE 1
Properties of Toluene and *n*-Octane at 15–20°C[a]

	Toluene	*n*-Octane
Molecular weight (g/mol)	92.14	114.23
Density (g/mL)	0.8716	0.7025
Aqueous solubility (mg/L)	515	0.67
Henry's constant (dimensionless)	0.2081	131
(Mass O^2)/(Mass VOC) in combustion	3.126	3.502

[a] Data calculated from Refs. 18 and 19.

Default values of the parameters used in modeling the biosparging of toluene and *n*-octane are given in Table 2. Parameters already listed in Table 1 are omitted.

The results are presented as individual runs in which the reduced residual VOC mass [$M_{tot}(t)/M_{tot}(0)$, the reduced vapor-stripped mass [$M_{vap}(t)/M_{tot}(0)$], and the reduced mass of biodegraded VOC [$M_{bio}(t)/M_{tot}(0)$] are plotted against time. Curves labeled *V* refer to vapor stripped VOC; curves labeled *B* to VOC destroyed by biodegradation. Unlabeled curves pertain to residual VOC.

The effects of variations in the dispersion D_s on the biosparging of toluene are seen in Fig. 3. The plots of reduced total residual contaminant mass $M_{tot}(t)/M_{tot}(0)$ show the expected increase in total removal rate as the dispersion is increased. The effect, however, is not large, leading us to conclude that dispersion transport is only one of the significant limiting factors here. The amounts of toluene removed by air stripping are nearly the same for the four cases shown, but there is a very substantial increase in the amount of toluene which undergoes biodegradation as increased dispersion coefficients permit increased oxygen transfer.

The effects of increases in the diffusivity of toluene in the boundary layer surrounding the NAPL droplets are seen in Fig. 4. Experimentally, one has no control over the diffusivity, but the model permits one to vary it to explore the extent to which diffusion-limited droplet solution rate controls the rate of NAPL removal. The total rate of cleanup [measured by $M_{tot}(t)/M_{tot}(0)$] undergoes a very marked increase as D_f increases from 0.5 to 2.0 $\times$ 10^{-10} m^2/s, as does the rate of toluene removal by stripping. The rate of biodegradation appears to be less affected. Evidently under these conditions the rate of solution of NAPL toluene is a major limiting factor for remediation. As D_f increases from 2.0 to 8.0 $\times$ 10^{-10} m^2/s, the total rate of cleanup and the rate of air stripping increase somewhat, but in this range the rate of NAPL droplet solution is sufficiently rapid that it is no longer the major rate-limiting step.

TABLE 2
Default Values of the Parameters Used in Modeling the Sparging of Toluene and *n*-Octane

Length of column	4 m
Diameter of column	0.2 m
Diameter of air channel	1.0 cm
Soil porosity	0.4
Soil density	1.7 g/cm^3
K_u, rate constant for biomass generation	1×10^{-5} s^{-1}
k_{die}, die-off rate constant	1×10^{-8} s^{-1}
B_0, Monod biomass parameter	100 mg/kg of soil
O_0, Monod oxygen parameter	1 mg/L of water
S_0, Monod substrate parameter (toluene, *n*-octane)	100, 1 mg/L of water
S_1, substrate inhibition parameter (toluene, *n*-octane)	2000, 5 mg/L of water
n, exponent in inhibition term	3
n_s, mass substrate/mass biomass	2
n_0, mass oxygen/mass (toluene, *n*-octane)	6.26, 7.00
D_f, substrate diffusivity	2×10^{-10} m^2/s
D_s, dispersivity	2×10^{-7} m^2/s
a_d, initial NAPL droplet diameter (toluene, *n*-octane)	0.1, 0.01 cm
b, droplet boundary layer thickness (toluene, *n*-octane)	0.5, 0.05 cm
Initial NAPL concentration (toluene, *n*-octane)	200, 1 mg/kg of soil
Initial dissolved VOC concentration (toluene, *n*-octane)	100, 0.5 mg/L of water
Initial biomass	0.005 mg/kg of soil
Initial dissolved oxygen concentration	0.0 mg/L of water
K_{H0}, Henry's constant of oxygen	33
q_{air}, air flow rate	10 mL/min
n_z, number of volume elements representing column	4
n_r, number of annular domains	6
Δt	100 seconds
t_{max}	50 days

Figure 5 shows the effect of the air flow rate through the channel, q_{air}. At the lower air flow rates (2 and 5 mL/min) both biodegradation and stripping are limited by the air flow rate, so they increase with increasing air flow. At the higher air flow rates (10 and 20 mL/min) the effect of a doubling of q_{air} is very markedly reduced, indicating that at these air flow rates the system is limited only slightly by the air flow rate. At the higher air flow rates the fraction of the toluene which is biodegraded decreases, as expected. Evidently, excessively high air flow rates should in general be avoided to reduce the costs for air pumping and for removing a larger quantity of VOC from a larger flow of gas in the off-gas treatment system.

In Fig. 6 we see the effect of increasing K_u, the effective first-order rate constant for biomass formation. As K_u increases, the rate of cleanup

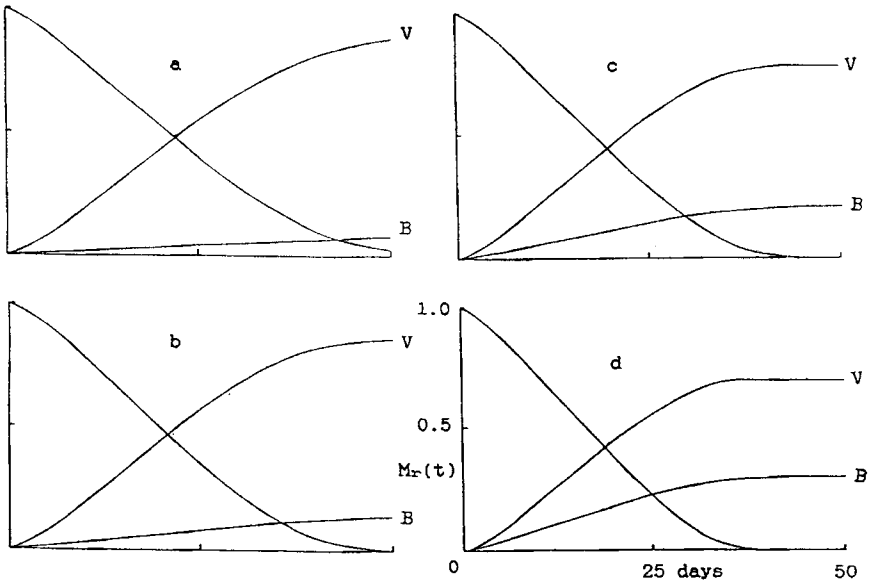

FIG. 3 Biosparging of toluene; effect of dispersivity D_s. Plots of reduced residual contaminant mass, vaporized contaminant mass, and biodegraded contaminant mass. D_s = (a) 0.25, (b) 0.5, (c) 1.0, and (d) 2.0×10^{-7} m^2/s. Other parameters as in Tables 1 and 2. B and V refer to the masses of contaminant removed by biodegradation and volatilization, respectively. The curve which decreases with increasing time is a plot of the reduced total contaminant mass in this and all subsequent figures.

of the system increases and the fraction of the toluene which is removed by biodegradation increases very substantially. At the air flow rate used in these runs (10 mL/min) the system is not oxygen-limited even at the highest rate of biodegradation. At the higher biodegradation rates the quantity of VOC in the off-gas which must be treated is very markedly reduced, so such increased rates are generally highly desirable. Possible means of achieving higher biodegradation rates include addition of nutrients such as fixed nitrogen and phosphorus, inoculation with special strains of microorganisms, and warming of the system. Unfortunately, some of these approaches present problems which have not yet been solved, although addition of nitrogen and phosphorus is not difficult.

We next turn to the biosparging of *n*-octane, the aqueous solubility of which is 0.67 mg/L (about 1/770th that of toluene), and the Henry's constant of which is 131 (about 630 times that of toluene). The large Henry's constant of *n*-octane makes its stripping an easy matter, provided that

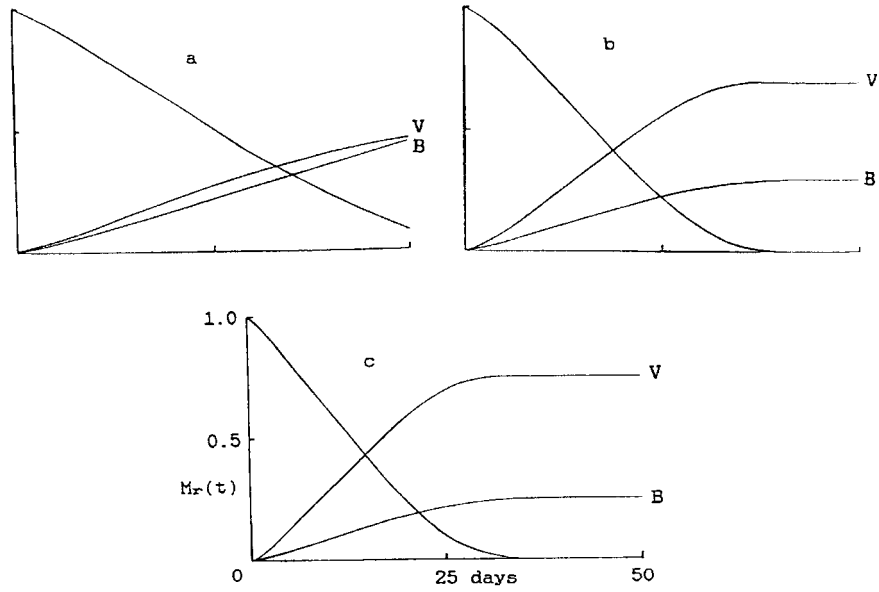

FIG. 4 Biosparging of toluene; effect of diffusivity D_f of toluene. D_f = (a) 0.5, (b) 2.0, and (c) 8.0×10^{-10} m^2/s. Other parameters as in Tables 1 and 2.

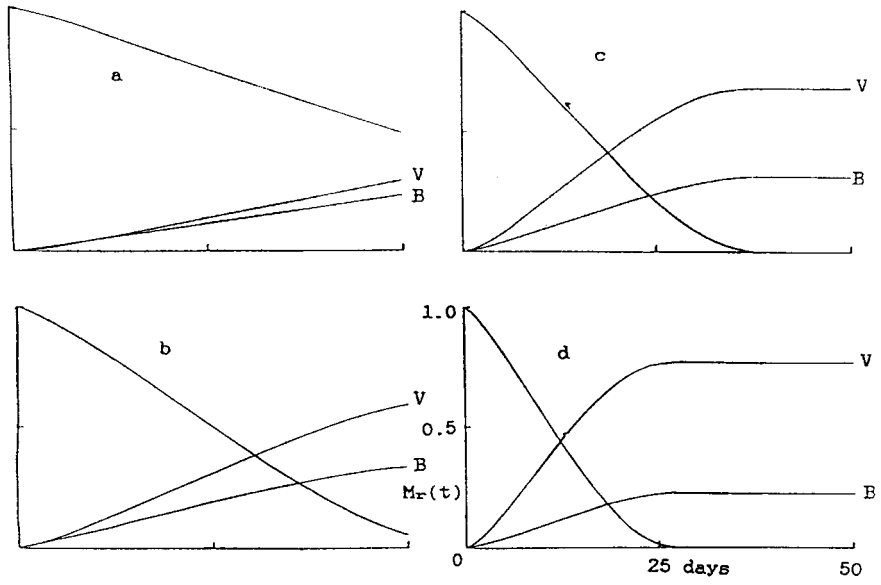

FIG. 5 Biosparging of toluene; effect of air flow rate. q_{air} = (a) 2, (b) 5, (c) 10, and (d) 20 mL/min. Other parameters as in Tables 1 and 2.

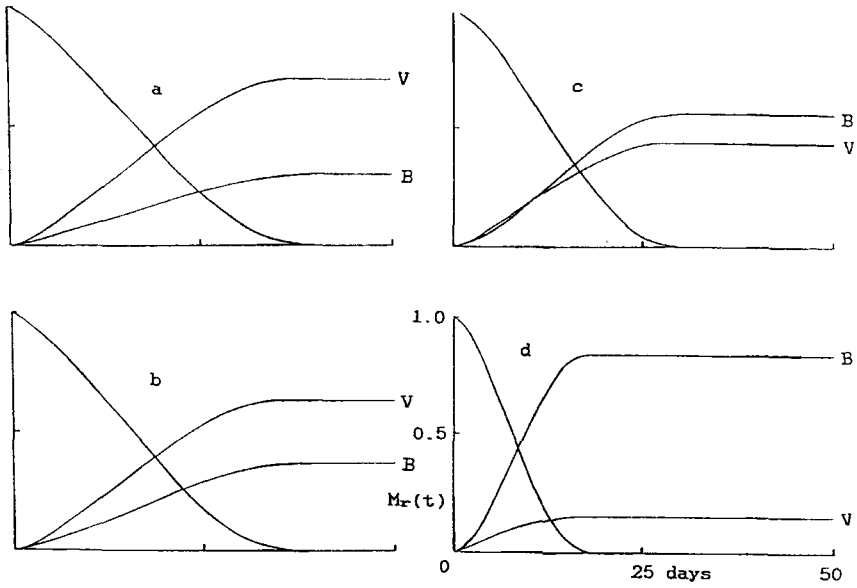

FIG. 6 Biosparging of toluene; effect of biodegradation rate parameter K_u. K_u = (a) 1.0, (b) 2.5, (c) 5.0, and (d) 10.0 $\times$ 10^{-5} s^{-1}. Other parameters as in Tables 1 and 2.

one is dealing only with dissolved VOC. On the other hand, inspection of Eq. (1) (which controls the rate of solution of NAPL droplets in water) or of Eq. (2) (which calculates the cleanup time for NAPL solution rate-limited systems) shows that this rate of solution is roughly proportional to the aqueous solubility of the VOC being dissolved. We therefore expect the very low solubility of *n*-octane to make the removal of NAPL by sparging and also by biosparging a very slow business.

The runs simulating the biosparging of *n*-octane shown in Fig. 7 show the magnitude of this effect. In these runs the NAPL droplet diameter and the boundary layer thickness are 0.1 and 0.5 cm, the same as used in the above toluene simulations. The diffusivity, D_f, is given values of 2×10^{-10}, 2×10^{-9}, and 2×10^{-8} m^2/s, equal to the default value used in the toluene simulations, ten times this value, and one hundred times this value. In all cases we see an initial very rapid rate of removal as dissolved VOC is stripped and biodegraded. In Figs. 7(a) and 7(b) this is followed by a long plateau region in which the rates of *n*-octane stripping and biodegradation are extremely slow, limited by the very low rate of solution of the NAPL droplets. Only when the diffusivity has been increased 100-fold above what are reasonable values do we see acceptable

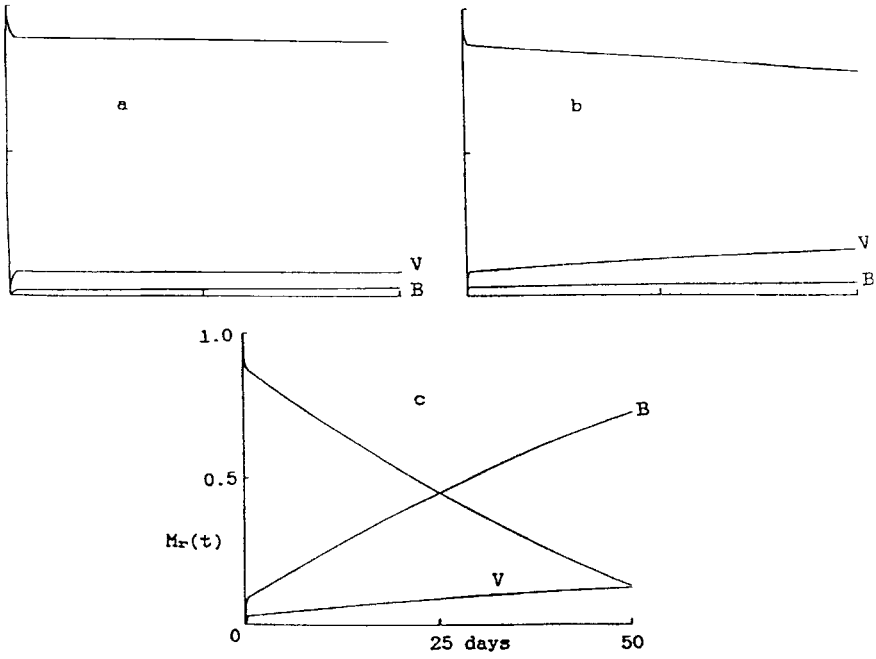

FIG. 7 Biosparging of *n*-octane; effect of diffusivity of *n*-octane. D_f = (a) 2.0×10^{-10}, (b) 2.0×10^{-9}, and (c) 2.0×10^{-9} m²/s; initial NAPL droplet diameter = 0.1 cm; boundary layer thickness b = 0.5 cm. Other parameters as in Tables 1 and 2.

cleanup rates for these systems. Obviously there is no hope of achieving such diffusivities.

This leads us to the unpleasant conclusion that it will be extremely difficult to remove or biodegrade alkanes (which are of quite low solubility) from smear zones which are beneath the water table at the time that sparging or biosparging is done. A possible solution to the problem is to draw down the water table in the vicinity of the sparging well by pumping to permit direct vaporization of the contaminant without the interposition of an aqueous boundary layer. Fortunately, the regulations are such that it is the BTEX and Total Petroleum Hydrocarbon concentrations which generally drive a remediation, and the BTEX compounds are relatively soluble. The problem is not so readily solved if one is dealing with DNAPLs such as tetrachloroethylene (solubility approximately 150 mg/L) or the dichlorobenzenes (solubilities in the 70–130 mg/L range), but these, although of relatively low solubility, are far more soluble than the

alkanes. The problem is exacerbated by the very low maximum concentration limits which have been set for most chlorinated solvents.

The effect of dispersivity on the biosparging of *n*-octane is seen in Fig. 8. The NAPL droplet size is 0.01 cm and the boundary layer thickness is 0.05 cm in these runs and those shown in Fig. 9. These were chosen to obtain illustrative displays, and are probably unrealistically small in most instances. The effect of dispersivity on the rate of cleanup is relatively slight, an expected result in view of the extent to which the rate of NAPL droplet solution is the limiting factor here. The rate of biodegradation is seen to increase somewhat with increasing D_s, presumably due to the increased dispersive transport of oxygen. It is apparent that efforts to increase the dispersivity by pulsed operation or any other technique will have little benefit if the VOC is below the water table and has a quite limited solubility. The very rapid removal of *n*-octane seen at the beginnings of these runs represents removal of the initially dissolved VOC.

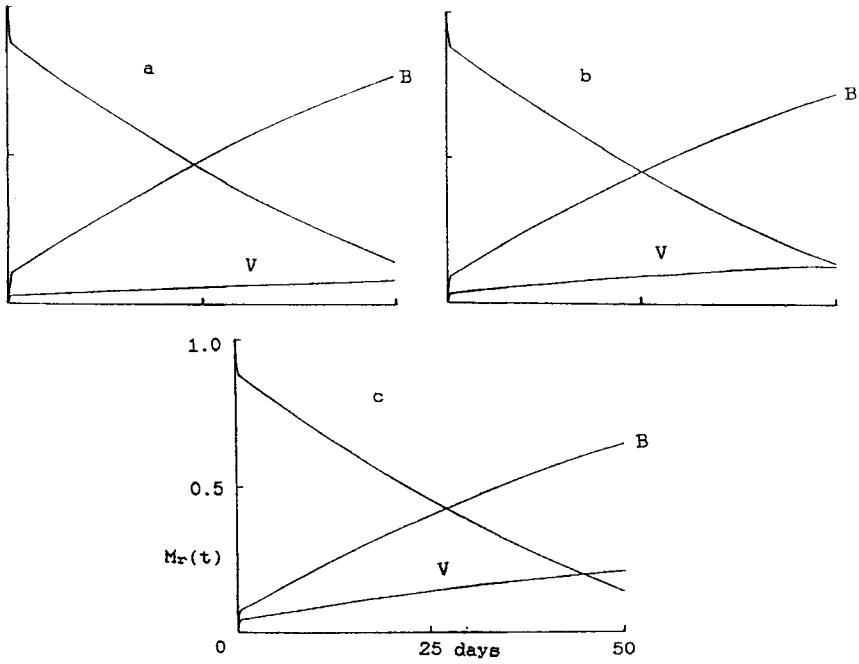

FIG. 8 Biosparging of *n*-octane; effect of dispersivity. D_s = (a) 1.0, (b) 2.0, and (c) 3.0 $\times 10^{-7}$ m^2/s; initial NAPL droplet diameter = 0.01 cm; boundary layer thickness b = 0.05 cm. Other parameters as in Tables 1 and 2.

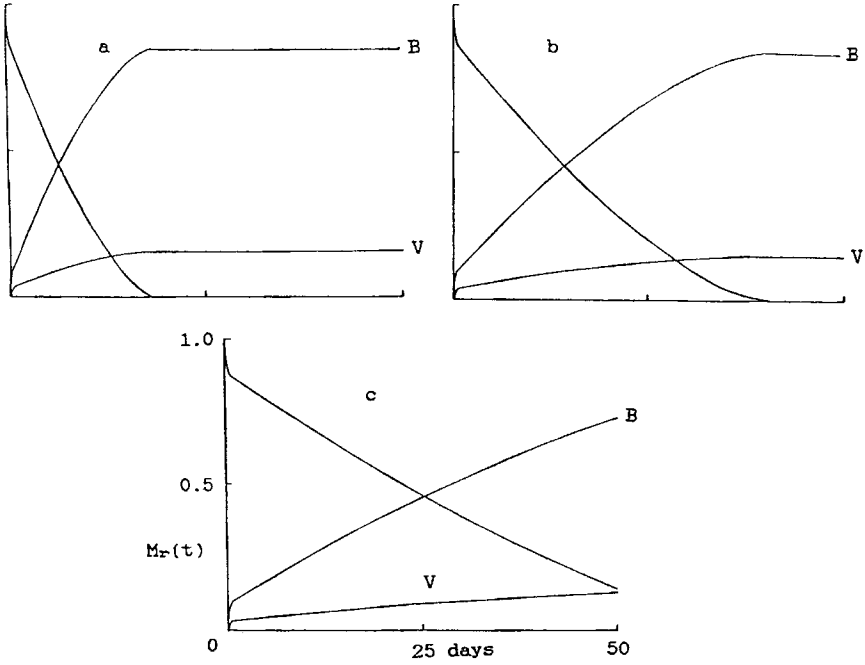

FIG. 9 Biosparging of *n*-octane; effect of initial NAPL droplet size a_0 and boundary layer thickness *b*. [a_0, b] = (a) [0.0050, 0.0250], (b) [0.0075, 0.0375], and (c) [0.0100, 0.0500] cm. Other parameters as in Tables 1 and 2.

The importance of NAPL droplet solution rates in the biosparging of *n*-octane is illustrated again by the simulations plotted in Fig. 9. In these runs the impact of droplet diameter/boundary layer thickness on cleanup rate is explored. Boundary layer thickness is assumed to be five times the initial droplet diameter, which is 0.0050, 0.0075, and 0.0100 cm. As droplet size increases, the water/NAPL interface decreases and the boundary layer thickness increases. Both of these cause a decrease in the rate of solution of the NAPL droplets, and a large decrease in cleanup rate results since the process is limited by the rate of droplet solution. These results suggest that one investigate techniques by which NAPL droplet size could be reduced. Speculative methods include 1) the use of ultrasonic energy to mechanically break up the droplets, and 2) the use of surfactants to reduce the surface tension of the NAPL–water interface, thereby making it easier to break up droplets by the shearing forces resulting from fluid flow during pulsed sparging.

CONCLUSIONS

The following conclusions can be drawn from our modelling work on biosparging.

- Dispersivities in the vicinity of a sparging well can be increased greatly by pulsed operation of the well. Short pulse cycles and high air injection pressures (limited by concern about blowout) yield the greatest increases in dispersivity, as shown by the arguments leading to Eq. (20).
- In situations involving relatively soluble VOCs such as BTEX, efforts spent enhancing the effective dispersivity of the system (by pulsed operation of the sparging well) are likely to markedly increase the rates of biodegradation and air stripping of VOC contaminants.
- Excessively low air flow rates result in excessively prolonged cleanups. Excessively high air flow rates result in excessive air pumping costs and off-gas treatment expenses, since large volumes of gas must be treated and relatively little VOC is biodegraded.
- The biosparging of NAPL VOCs of very low solubility (such as alkanes) which are trapped in smear zones below the water table is an extremely slow process due to the very slow rate of solution of the NAPL in the surrounding water. A possible solution is the lowering of the water table by pumping and by taking advantage of the annual water table fluctuations.
- The biosparging of NAPL VOCs of low solubility is accelerated if the size of the droplets is decreased. One speculates that sonication and/or surfactants might be effective for this.
- The biosparging of NAPL VOCs of very low solubility will not be significantly enhanced by pulsed operation of the sparging well unless the energy input and water currents induced are sufficient to break up the NAPL droplets. The prospects for this appear slim.
- Moderate increases in temperature, of the order of 10°C, would accelerate both the rate of solution of NAPL VOCs and the first-order rate constants for microbial processes.

REFERENCES

1. Committee on Groundwater Cleanup Alternatives, *Alternatives for Groundwater Cleanup*, National Academy Press, Washington, D.C., 1994.
2. R. A. Brown, "Sparging: a New Technology for the Remediation of Aquifers Contaminated with Volatile Organic Compounds," in *Modeling of In Situ Techniques for Treatment of Contaminated Soils: Soil Vapor Extraction, Sparging, and Bioventing* (D. J. Wilson, Ed.), Technomic Publishing Co., Lancaster, PA, 1995.
3. M. E. Loden, *A Technology Assessment of Soil Vapor Extraction and Air Sparging*,

US EPA Report EPA/600/R-92/173, Risk Reduction Engineering Laboratory, Office of Research and Development, US EPA, Cincinnati, OH, 1992.

4. R. E. Hinchee and S. K. Ong, "A Rapid In Situ Respiration Test for Measuring Aerobic Biodegradation Rates of Hydrocarbons in Soils," *J. Air Waste Manage. Assoc.*, *42*, 1305 (1992).
5. R. E. Hoeppel and R. E. Hinchee, "Enhanced Biodegradation for On-Site Remediation of Contaminated Soils and Groundwater," in *Hazardous Waste Site Soil Remediation: Theory and Application of Innovative Technologies* (D. J. Wilson and A. N. Clarke, Eds.), Dekker, New York, 1994.
6. J. S. Kindred and M. A. Celia, "Contaminant Transport and Biodegradation. 2. Conceptual Model and Test Simulation," *Water Resour. Res.*, *25*, 1149 (1989).
7. C. Gomez-Lahoz, J. J. Rodriguez, J. M. Rodriguez-Maroto, and D. J. Wilson, "Biodegradation Phenomena during Soil Vapor Extraction. III. Sensitivity Studies for Two Substrates," *Sep. Sci. Technol.*, *29*, 1275 (1994).
8. A. Leeson, R. E. Hinchee, and C. M. Vogel, *Evaluation of the Effectiveness of Air Sparging*, Presented at In Situ and On-Site Bioreclamation: The Third International Symposium, April 24–27, 1995, San Diego, CA.
9. M. A. Dahmani, D. P. Ahlfeld, G. E. Hoag, and W. Ji, *Field Behavior of Air Sparging: Implications of a Conceptual Model*, Presented at In Situ and On-Site Bioreclamation: The Third International Symposium, April 24–27, 1995, San Diego, CA.
10. D. H. Mohr, *Mass Transfer Concepts Applied to In Situ Air Sparging* Presented at In Situ and On-Site Bioreclamation: The Third International Symposium, April 24–27, 1995, San Diego, CA.
11. R. L. Johnson, N. R. Thomson, and P. C. Johnson, *Does Sustained Groundwater Circulation Occur during In Situ Air Sparging*, Presented at In Situ and On-Site Bioreclamation: The Third International Symposium, April 24–27, 1995, San Diego, CA.
12. F. C. Payne, A. R. Blaske, G. A. vanHouten, and J. B. Lisiecki, *Comparison of Contamination Removal Rates in Pulsed and Steady-Flow Aquifer Sparging*, Presented at In Situ and On-Site Bioreclamation: The Third International Symposium, April 24–27, 1995, San Diego, CA.
13. D. J. Wilson, C. Gomez-Lahoz, and J. M. Rodriguez-Maroto, "Groundwater Cleanup by In-Situ Sparging. VIII. Effect of Air Channeling on Dissolved Volatile Organic Compounds Removal Efficiency," *Sep. Sci. Technol.*, *29*, 2387 (1994).
14. D. J. Wilson, R. D. Norris, and A. N. Clarke, "Groundwater Cleanup by In-Situ Sparging. IX. Air Channeling Model for Nonaqueous Phase Liquid Removal," *Ibid.*, *31*, 915 (1996).
15. C. Gomez-Lahoz, J. M. Rodriguez-Maroto, and D. J. Wilson, *Determination of the Rate-Limiting Process for Bioventing*, Presented at In Situ and On-Site Bioreclamation: The Third International Symposium, April 24–27, 1995, San Diego, CA.
16. C. Gomez-Lahoz, J. M. Rodriguez-Maroto, and D. J. Wilson, "Biodegradation Phenomena during Soil Vapor Extraction: A High-Speed Nonequilibrium Model," *Sep. Sci. Technol.*, *29*, 429 (1994).
17. A. E. Scheidegger, *The Physics of Flow through Porous Media*, University of Toronto Press, Toronto, Canada, 1974.
18. D. R. Lide (Ed.), *Handbook of Chemistry and Physics*, 71st ed., CRC Press, Boca Raton, FL, 1990.
19. J. H. Montgomery and L. M. Welkom, *Groundwater Chemicals Desk Reference*, Lewis Publishers, Chelsea, MI, 1990.

Received by editor September 21, 1995